Accepted version.
Cite as: BE McKenzie, F Nudelman, PHH Bomans, SJ Holder, NAJM Sommerdijk, *Journal of the American Chemical Society* 132 (30), 10256-10259.
DOI: 10.1021/ja102040u

Temperature responsive nanospheres with bicontinuous internal structures from a semi-crystalline amphiphilic block copolymer

Beulah E. M[c]Kenzie[a], Fabio Nudelman[b], Paul H.H. Bomans[b], Simon J. Holder[a]*, Nico A. J. M. Sommerdijk[b]*

[a] *Functional Materials Group, School of Physical Sciences, University of Kent, Canterbury, Kent. CT2 7NH. UK.*
[b] *Laboratory of Materials and Interface Chemistry and Soft Matter Cryo-TEM Research Unit, Eindhoven University of Technology, PO Box 513, 5600 MB, Eindhoven, The Netherlands.*

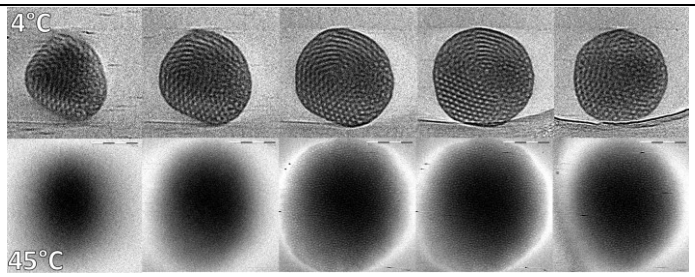

Internally structured self-assembled nanospheres, cubosomes, are formed from a semi-crystalline block copolymer, poly(ethylene oxide)-*block*-poly(octadecyl methacrylate) (PEO_{39}-b-$PODMA_{17}$), in aqueous dispersion. The poly(octadecyl methacrylate) block provides them with a temperature responsive structure and morphology. Using cryo-electron tomography, we show that at room temperature these internally bicontinuous aggregates undergo an unprecedented order-disorder transition of the microphase separated domains that is accompanied by a change in the overall aggregate morphology. This allows switching between spheres with ordered bicontinuous internal structures at temperatures below the transition temperature and more planar oblate spheroids with a disordered microphase-separated state above the transition temperature. The bicontinuous structures offer a number of possibilities for application as templates e.g. for biomimetic mineralisation or polymerization. Furthermore, the unique nature of the thermal transition observed for this system offers up considerable possibilities for their application as temperature-controlled release vessels.

Temperature responsive nanospheres with bicontinuous internal structures from a semi-crystalline amphiphilic block copolymer

Beulah E. M[c]Kenzie[a], Fabio Nudelman[b], Paul H.H. Bomans[b], Simon J. Holder[a]*, Nico A. J. M. Sommerdijk[b]*

[a] *Functional Materials Group, School of Physical Sciences, University of Kent, Canterbury, Kent. CT2 7NH. UK.*
[b] *Laboratory of Materials and Interface Chemistry and Soft Matter Cryo-TEM Research Unit, Eindhoven University of Technology, PO Box 513, 5600 MB, Eindhoven, The Netherlands.*

RECEIVED DATE (automatically inserted by publisher); S.J.Holder@kent.ac.uk; N.Sommerdijk@tue.nl

Amphiphilic AB and ABA block copolymers have been demonstrated to form a variety of self-assembled aggregate structures in dilute solutions where the solvent preferentially solvates one of the blocks.[1] The most common structures formed by these amphiphilic macromolecules are spherical micelles, cylindrical micelles and vesicles (polymersomes), with the type of aggregate depending principally upon the relative volumes of the different blocks.[1] Over the past decade more complex aggregate structures have been observed and targeted for construction. The majority of these aggregates (such as disk-like and toroidal micelles) may be grouped under the description of complex micelles and can be achieved both through manipulating block copolymer structures and through physical means.[2] Multi-compartment micelles are typically the result of ABC block copolymers, of which one of the blocks is solvophilic and the remaining two are solvophobic but do not mix.[3] Hence microphase separated micellar cores result.

We recently reported the experimental observation of complex micelles with bicontinuous hydrophilic/hydrophobic internal structures from amphiphilic norbornene-based double-comb diblock copolymers, with peptide and oligo(ethylene oxide) side chain.[4] Block copolymer nanoparticles with similar bicontinuous phase separation have also been observed by Wooley et al, [5] and before that were predicted by Fraaije and Sevink.[6] In the present paper we demonstrate the formation of similar complex micelles, with hydrophobic bicontinuous internal morphologies from an amphiphilic semi-crystalline AB(C) comb-like block copolymer. Using cryo-electron tomography, we show that at room temperature these internally structured nanoparticles undergo an unprecedented order-disorder transition involving the reorganization of the microphase separated domains that is accompanied by a change in the overall aggregate morphology.

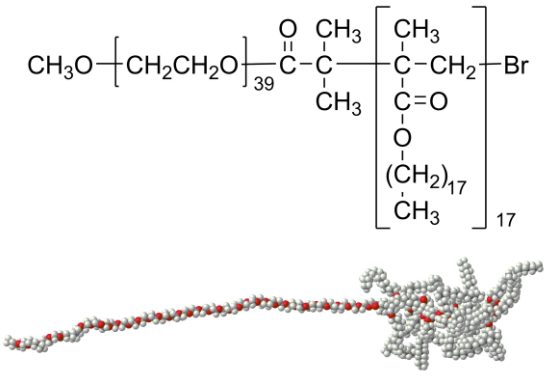

Scheme 1. Chemical structure (top) and 3D represenatation (bottom) of PEO_{39}-b-$PODMA_{17}$

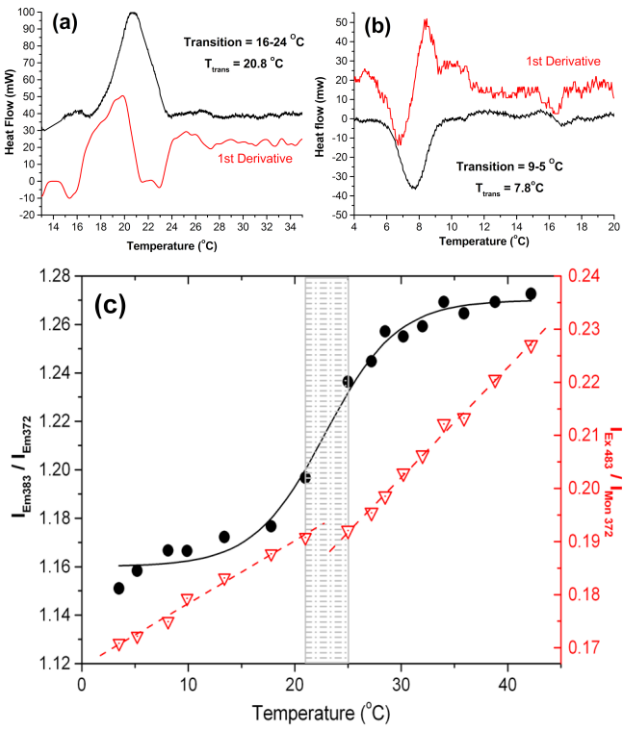

Figure 1. DSC traces of 5 wt% solution of PEO-PODMA aggregates 10K min^{-1} (a) heating run, (b) cooling run; (c) variation with temperature of ratios of the III:I (I_{Em383}/I_{Em372}) bands and the I_{exc}:I_{mon} (I_{Ex483}/I_{Mon372}) bands for pyrene encapsulate din 1 wt% aggregate solutions.

A new AB(C) amphiphilic block copolymer, poly(ethylene oxide)-block-poly(octadecyl methacrylate) (PEO_{39}-*b*-$PODMA_{17}$, M_n 7,680; M_w/M_n = 1.11, $W\%_{PEO}$ 25) was synthesized by the atom transfer radical polymerisation of octadecyl methacrylate from a poly(ethylene oxide) macroinitiator (SI, SI). DSC studies showed two melting transitions for the bulk material: the first at 24.2°C (PODMA), and the second at 31.3°C (PEO) (SI). Aggregate dispersions of this copolymer were formed by slow addition of 6 ml of water to 4ml THF solutions at 35°C and subsequent dialysis against water at 35°C over 24 hours to give 1 wt% and 5 wt% aggregate dispersions in 10 ml water (SI).[7] The initial solutions went from transparent to white translucent during water addition indicating preliminary aggregation of the copolymer during this process; the solutions became opaque white during subsequent dialysis. Negative staining transmission electron microscopy (TEM) demonstrated that at room temperature spherical aggregates were present with diameters of

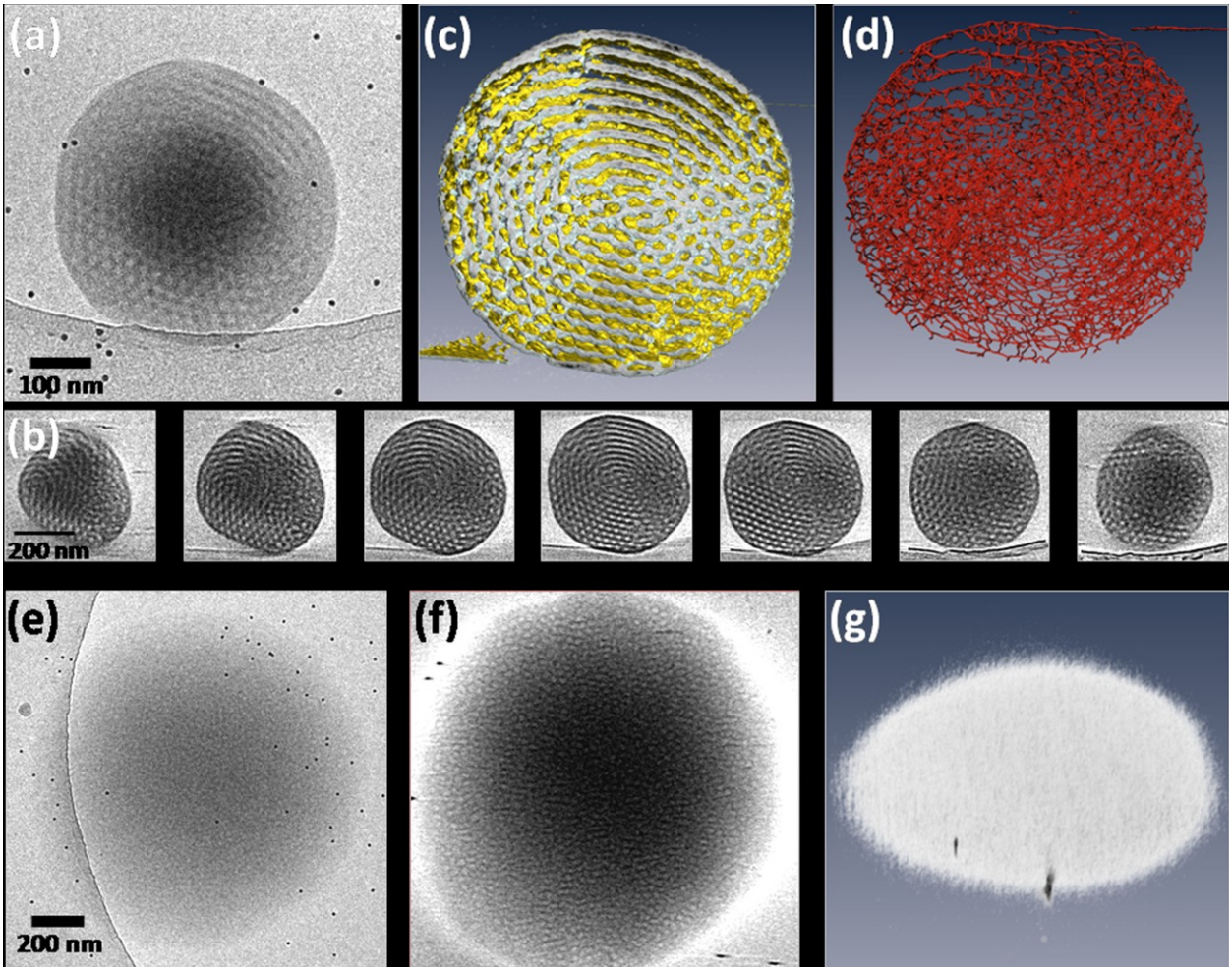

Figure 2. TEM analysis of PEO_{39}-*b*-$PODMA_{17}$ aggregates: (a) cryoTEM image of a vitrified film at 4°C; (b) gallery of z slices showing different cross sections of a 3D SIRT (simultaneous iterative reconstruction technique) reconstruction of a tomographic series recorded from the vitrified film in (a); (c) computer-generated 3D visualization showing only an inner section of the whole structure, where all the channels and compartments are visible (the yellow surface is outside of the polymer, the surface in contact with the water); (d) skeletonization of (c), showing only a small section emphasizing that the structure is interconnected and therefore bi-continuous; (e) cryoTEM image of a vitrified film at 45°C; (f) slice from a 3D SIRT (simultaneous iterative reconstruction technique) reconstruction of a tomographic series recorded from the vitrified film in (e); (g) volume rendering of the whole structure in (e), showing the overall morphology.

200±100 nm for the 1 wt% and 450±150 nm for the 5wt% solutions (SI). DLS studies of the solutions at 35°C gave number average diameters of 343 nm (dispersity = 0.366) for the 5wt% and 276nm (dispersity = 0.310) for the 1wt%. DSC analysis of the 5 wt% solution revealed an endothermic thermal transition with a T_{trans} = 21.8°C on heating and a T_{trans} = 7.8°C on cooling (peak maxima, Fig 1a, 1b). These transitions are tentatively assigned to the melting and crystallisation of portions of the octadecyl chains in the aggregates.[8]

The structure and the thermal behaviour of these aggregates was further investigated with cryoTEM and cryo-electron tomography (cryoET - 3D cryoTEM). The 2D cryoTEM projection images of the 5wt% solution vitrified 4°C showed numerous round aggregates that possessed an ordered internal microphase-separated structure (Fig. 2a, SI Fig S10a,S11). Samples vitrified at the transition point (22°C) showed spherical aggregates with a variety of internal structures with lower apparent order compared to the those present at 4°C (SI Fig. S10b,S12). Also the projection images recorded at 45°C showed round objects however these showed poor contrast with the surrounding vitrified ice matrix and an ordered internal structure could no longer be observed (Fig. 2e, SI Fig S10c, S13). CryoET was performed by recording tilt series of 85-95 cryoTEM images of the vitrified samples between -70° and +70° with increments of 2° at low angles and 1° at high angles and subsequently reconstructing the investigated volume using a SIRT algorithm (Fig 2b). The 3D visualization of the reconstructed volumes revealed that below T_{trans} the aggregates were spherical and predominantly possessed a sponge-like structure, consisting of an ordered bicontinuous network of intertwined water-filled and carbon-rich channels (both ~13nm in thickness/diameter), in which the aqueous channels were in contact with the surrounding medium (Fig. 2c, 2d, S15). Whilst the majority structural component of the aggregates at 4°C was observed to be bicontinuous some internal lamellar organisation was observed in places (Fig. 2c). Whilst the origin of the lamellar regions remains unknown it's coexistence with the bicontinuous morphology suggests that the aggregates internal structure may lie at a hypothetical phase boundary between the two microphase separated states.[9] The tilt series (Fig. 2f, SI, Fig. S14) and 3D reconstructions (Fig. 2g) of the aggregates at 45°C still showed some residual but highly disordered microphase separated structure (again with ~13nm dimensions) in the interior of aggregates vitrified at temperatures above T_{trans}. These 3D images

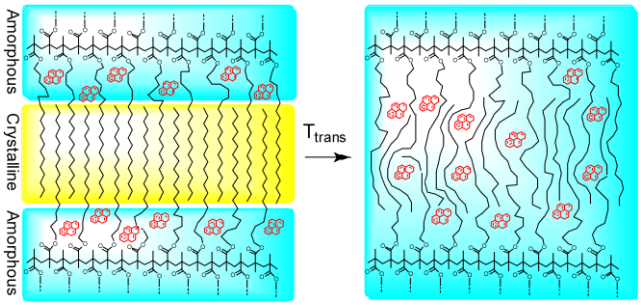

Figure 3. Schematic representation of the melting of the crystalline portions of the octadecyl chains and the concomitant changes in the pyrene environment

also revealed that the aggregates were not spherical but had a flattened, oblate spheroidal shape.

In line with DSC data obtained for solution and bulk samples of the block copolymer we suggest that above T_{trans} an order-disorder transition is taking place that accompanies the melting of the octadecyl chains. Furthermore, the tomograms showed that during the thermal transition the aggregates flatten to a more planar oblate spheroid morphology which, along with the now completely amorphous nature of the block copolymer explains the reduced electron density observed in the 2D images. Unfortunately the resolution and contrast of the reconstructions did not allow us to determine whether the observed residual compartments were interconnected throughout the interior of the aggregates, as was the case below T_{trans}. CryoTEM and cryoET of the 1 wt% solution above and below T_{trans} gave similar results to those observed for the 5wt% solution although the degree of order at 4°C and the microphase separation at 45°C were less pronounced (SI Fig. S8, S9).

Variable temperature fluorescence spectroscopy of a 1 wt% aggregate solution containing encapsulated pyrene (py) revealed marked changes in the intensities of both the py monomer signals (I_{mon}) and the excimer peak (I_{exc}) in the temperature range of 17-25°C (Fig 1c, SI Fig S18), indicating significant changes in the environment of the probe molecues.[10] The transition in this temperature range closely matches that observed by DSC for the 5 wt% solution The mid-point of the I_{III}/I_I sigmoidal plot is 22.9°C and the intersection of the slopes for the I_{exc}/I_{mon} plot is 23.1°C (Fig 1c). Both values are very close to the T_{trans} of 21.8°C providing confirmation for a change in structure of the microphase separated state deduced from the observed transition temperature recorded by DSC and images from TEM. The increase in the pyrene I_{III}/I_I ratio from ~ 1.16 to 1.26 indicates a decrease in the polarity (an increase in the hydrophobicity) of the environment of the probe.[11,12] The change in the slope of the I_{exc}/I_{mon} *vs* T plot at ~ 22-25°C (Fig. 2c) is indicative of a decrease of the micro-viscosity in the py environment.[10,13] Since py is excluded from the crystalline portions of semi-crystalline polymers these observations support the postulate that at T_{trans} upon heating, the crystalline segments of the octadecyl chains melt resulting in py dilution in the chains and reduced proximity to the polar C=O groups (Fig. 3).[14] The resultant entirely amorphous PODMA phase will have an increased hydrophobicity in agreement with the observed increase in I_{III}/I_I ratio. This leads to a higher probe mobility as associated with the semi-crystalline-to-amorphous transition in the polymer, and in line with the more rapid increase of the I_{exc}/I_{mon} ratio observed in the temperature range of 22-25°C. Whilst the presence of crystalline regions is not needed for the formation of these large microphase separated aggregates (given that they are formed at 35°C) it would appear that a degree of crystallinity is necessary for the formation of the bicontinuous morphology.

These internally structured self-assembled nanospheres that were only recently observed for the first time can be considered the polymeric analogues of cubosomes, aggregates that exhibit interior bicontinuous liquid crystalline order. Typically cubosomes are formed from low molecular weight compounds that are often present as mixtures and often require stabilisers.[15] These polymer cubosomes are now formed from a semi-crystalline block copolymer which provides them with temperature responsive structure and morphology. This allows switching between spheres with ordered bicontinuous internal structures at temperatures below the transition point and disc-like structures with a disordered microphase separated internal composition above. The bicontinuous structures offer a number of possibilities for application as templates e.g. for biomimetic mineralisation or polymerization. Furthermore, the unique nature of the thermal transition observed for this system offers up considerable possibilities for their application as temperature-controlled release vessels.

Supporting Information Available: SI1 Experimental: Scheme 1; Figs. S1-S5; Table SI1. SI2 DSC: Figs. S7. SI3 DLS: Figs. S7. SI4 CryoTEM: Figs. S8-S16. SI5 Fluorescence: Figs. S17-S19.

REFERENCES

1. (a) Tuzar, Z.; Kratochvil, P; In: Matijevic E; editor. Surface and Colloid Science, vol. 15. New York: Plenum Press 1993. pp.1. (b) Discher, B. M.; Hammer D. A.; Bates F. S.; Discher D.E. *Curr. Opin. Colloid. In. Sci.* **2000**, *5*, 125-131. (h) Zhang, L.; Eisenberg, A. *Polym. Advan. Technol.* **1998**, *9*, 677-699. (k) Lutz, J. F. *Polym. Int.* **2006**, *55*, 979-993. (l) Gohy, J. F. *Adv. Polym. Sci.* **2005**, *190*, 65-136.
2. (a) Chen, Z. Y.; Cui, H. G.; Hales, K.; Li, Z. B.; Qi, K.; Pochan, D. J.; Wooley, K. L.; *J. Am. Chem. Soc.* **2005**, *127*, 8592-8593 (b) Pochan, D. J.; Chen, Z. Y.; Cui, H. G.; Hales, K.; Qi, K.; Wooley, K. L.; *Science* **2004**, *306*, 94-97 (c) Yu, H. Z.; Jiang, W.; *Macromolecules* **2009**, *42*, 3399-3404 (d) Li, Z. B.; Chen, Z. Y.; Cui, H. G.; Hales, K.; Qi, K.; Wooley, K. L.; Pochan, D. J. *Langmuir* **2005**, *21*, 7533-7539 (e) Gomez, E. D.; Rappl, T. J.; Agarwal, V.; Bose, A.; Schmutz, M.; Marques, C. M.; Balsara, N. P. *Macromol.* **2005**, *38*, 3567-3570
3. (a) Li, Z. B.; Kesselman, E.; Talmon, Y.; Hillmyer, M. A.; Lodge, T. P. *Science* **2004**, *306,* 98-101. (e) Laschewsky, A.; *Curr. Opin. Colloid. In. Sci.* **2008**, *8*, 274-281 (c) Lutz, J-F.; Laschewsky, A.; *Macro. Chem. Phys.* **2005**, *206*, 813-817 (d) Weberskirch, R.; Preuschen, J.; Spiess, H. W.; Nuyken, O. *Macro. Chem. Phys.* **2000**, *201*, 995-1007. (e) H. Yabu, T. Higuchi, M. Shimomura, *Adv. Mater*. 2005, 17, 2062. (f) M. Okubo, R. Takekoh, N. Saito, *Colloid Polym Sci* 2004, 282, 1192. (g) N. Saito, R. Takekoh, R. Nakatsuru, M. Okubo, *Langmuir* 2007, 23, 5978. (h) H. Cui, Z. Chen, S. Zhong, K. L. Wooley, D. J. Pochan *Science* **2007**, 317, 647.
4. (a) Parry, A. L.; Bomans, P. H. H.; Holder, S. J.; Sommerdijk, N. A. J. M.; Biagini, S. C. G. *Angew. Chem. Int. Ed.* **2008**, *47*, 8859-8862.
5. X. Hales, K.; Chen, Z.; Wooley, K.L.; Pochan, D.J. *Nano Letters*, **2008**, 8, 2023.
6. Fraaije J.G.E.M., Sevink G.J.A. Macromolecules **2003**, 36, 7891-7893.
7. (a) Holder, S.J., Durand, G.G., Yeoh, C-T., Illi, E., Hardy, N.J., Richardson, T.H., *J Polym Sci Pt A: Polym Chem* **2008**, 46, 7739-7756. (b) Holder, S.J., Rossi, N.A.A., Yeoh, C-T., Durand, G.G., Boerakker, M.J., Sommerdijk, N.A.J.M, *J Mater Chem* **2003**, 13, 2771 – 2778.
8. Hempel E., Budde H., Horing S., Beiner M. *J Non-Cryst Solids* **2006**, 352, 5013-5020.
9. Meuler A.J., Hillmyer M.A., Bates F.S. *Macromolecules* **2009**, 42, 7221-7250.
10. (a) Duportail, G.; Lianos, P. In *Vesicles*; Rosoff, Ed. Dekker, M.: New York, **1996**, 295-372 (b) Metso, A. J.; Jutila, A.; Mattila, J-P.; Hlopainen, J. M.; Kinnunen, P. K. J. *J. Phys. Chem. B* **2003**, *107*, 1251-1257 (c) Jung, M.; Hubert, D. H. W.; van Veldhoven, E.; Frederik, P. M.; Blandamer, M. J.; Briggs, B.; Visser, A. J. W. G.; van Herk, A. M.; German, A. L. *Langmuir* **2000**, *16*, 968-979.
11. Waris, R.; Acree Jr., W. E.; Street, K. W. *Analyst* **1988**, *113*, 1465-1467.
12. Kalyanasundaram, K.; Thomas, J. K. *J. Amer. Chem. Soc.* **1977**, 99, 2039-2044.
13. Aoudia, M.; Rogers, M. A. J.; Wade, W. H. *J. Phys. Chem.* **1984**, 88, 5008-5012.
14. Vigil, M. R.; Bravo, J.; Atvars, T. D. Z.; Baselga, J. *Macromolecules* **1997**, *30*, 4871-4876.
15. (a) Larsson, K. *J. Phys. Chem.* **1989**, *93*, 7304-7314. (b) Larsson, K. *Curr. Opin. Colloid Interface Sci*. **2000**, *5*, 64-69. (c) Bucheim, W.; Larsson, K. *J. Colloid Interface Sci*. **1987**, *117*, 582-583.(d) Larsson, K. *J. Phys. Chem*. **1989**, *93*, 7304-7314. (e) Landh, T. *J. Phys. Chem*. **1994**,

98, 8453-8467. Spicer, P. T. *Curr. Opin. Colloid Interface Sci.* **2005**, *10*, 274. Barauskas, J.; Johnsson, M.; Tiberg, F. *Nano Lett.* **2005**, *5*, 1615. (f) Barauskas, J.; Johnsson, M.; Joabsson, F.; Tiberg, F. *Langmuir* **2005**, *21*, 2569.

Supporting Information

Temperature responsive nanospheres with bicontinuous internal structures from a semi-crystalline amphiphilic block copolymer

Beulah M[c]Kenzie[a], Fabio Nudelman[b], Paul H.H. Bomans[b], Simon J. Holder[a]*, Nico A. J. M. Sommerdijk[b]*

[a] *Functional Materials Group, School of Physical Sciences, University of Kent, Canterbury, Kent. CT2 7NH. UK.*
[b] *Laboratory of Materials and Interface Chemistry and Soft Matter Cryo-TEM Research Unit, Eindhoven University of Technology, PO Box 513, 5600 MB, Eindhoven, The Netherlands.*

Contents

Supporting Information

SI1 Experimental

Materials and Apparatus

Poly (ethylene glycol) methyl ether (molecular weights ca. 2000 $gmol^{-1}$), 2-bromoisobutyryl bromide (98%), dimethylamino pyridine (99%), triethylamine (99%), octadecyl methacrylate (ODMA) and copper (I) bromide (98%) were all purchased without further purification from Sigma-Aldrich. Aluminium oxide (activated, neutral, for column chromatography 50-200μm) and magnesium sulphate (97%, anhydrous) were purchased from Acros Organics. Sodium bicarbonate (analytical reagent grade) was purchased from Fisher Scientific. Hydrochloric acid (35.4%; sp. gr. 1.18) was purchased from BDH Chemicals. N-(n-octyl)-2-pyridyl(methanime) was synthesised according to literature[1].

Methanol (analytical reagent grade), tetrahydrofuran (analytical reagent grade), isopropanol, ethanol (analytical reagent) and water (HPLC gradient grade) were all purchased from Fisher Scientific. Dichloromethane (analytical reagent grade) was purchased from Fisher Scientific, and before use was dried and distilled over calcium hydride. σ xylene was purchased from BDH Lab Supplies. The deuterated solvent D_1-chloroform (99.8%) was used as received from Cambridge Isotope Laboratories Incorporated.

Characterisation

^{1}H NMR spectra were recorded using a JEOL GX-270 FT spectrometer (270 MHz) at 25˚C in solutions of deuterated chloroform ($CDCl_3$). ^{1}H NMR was used to ascertain structure and follow monomer conversion of the polymers. Molecular weight averages were calculated via size exclusion chromatography (SEC) using two 5μm mixed C PLgel columns at 40˚C, calibrated using poly(methyl methacrylate) standards. The samples in THF were detected by a Shodex RI-101 refractive index detector. Infra-red spectra were collected using a Thermo Nicolet Avatar 360 FT-IR spectrometer.

Thermal Analysis

A Perkin Elmer differential scanning calorimeter (PE DSC 7) calibrated with Indium (mp = 156.1, ΔH = 28.3 J/g) was used to determine the thermal energies of the block copolymers, at a scanning rate of 10^{o}C/min. The temperatures for melting and crystallisation were determined from the peak maxima of the heating and cooling curves.

Dialysis

10mg of block copolymer was dissolved in 4ml THF and left stirring in an oil bath at 35^{o}C. 6ml water was added drop-wise to the stirring solution over 90mins. The solution was transferred to dialysis tubing, sealed and immersed in 3 L of stirring 35^{o}C deionised water for 24 hours to displace the THF. During this time, the water was replaced twice. For fluorescence studies the block copolymer was dissolved in a $5x10^{-5}$ M solution of pyrene in THF, and the method followed as stated above.

Fluorescence

Excitation and emission spectra were collected using a Varian CARY Eclipse fluorescence spectrophotometer and a Perkin Elmer LS 50 B luminescence spectrometer.

Optical and Size Measurements

Transmission electron microscopy (TEM) was carried out using a JEOL JEM (200-FX) machine, operating at 120kV. 20μl of the dialysed sample was deposited onto a carbon-covered copper grid, left for 30s and removed via suction. The grid was then stained with a solution of 5% uranyl acetate and 1% acetic acid. 20μl of this solution was deposited on the grid and removed after 5s. Excess solution was dabbed away using filter paper. Dynamic light scattering (DLS) measurements were carried out on a Malvern High Performance Particle Sizer (HPPS HPP5001) with a laser at a wavelength of 633nm. 1ml

of the dialysed solution was taken, filtered using a 1.2 µm filter and placed in a clean cuvette. The desired temperature was set and the sample left at this temperature for 15mins before the runs were conducted. At each temperature ten size readings were obtained and an average of these taken.

CryoTEM

Sample vitrification was carried out on an automated vitrification robot (FEI Vitrobot^{TM} Mark III) for plunging in liquid ethane. CryoTEM Cu R2/2 Quantifoil Jena Grids (Quantifoil Micro tools GmbH) were surface plasma treated using a Cressington 208 carbon coater prior to use. For vitrification, 3 µl/ml of PEO_{39}-*b*-$PODMA_{17}$ (1 mg/ml in water), equilibrated to 4 ˚C or to 45 ˚C, was applied to the cryoTEM grids inside the vitrobot chamber which was conditioned to 100 % humidity and 4 ˚C or 45 ˚C.

For 2D imaging and tomography, samples were studied on the TU/e CryoTitan (FEI, www.cryotem.nl), equipped with a with a field emission gun (FEG) operating at 300 kV. Images were recorded using a 2k x 2k Gatan CCD camera equipped with a post column Gatan Energy Filter (GIF).

The 3-dimensional reconstructions were preformed with the software Inspect 3D v.3.0 (FEI Company). For the segmentation and visualization of the 3D volume, Amira 4.1.0 (Mercury Computer Systems) was used.

Supporting Information

Tomography conditions:

1wt% solution PEO_{39}-*b*-$PODMA_{17}$

PEO_{39}-*b*-$PODMA_{17}$ at 4 ˚C:

From -70° to +70°, with 2° increments from 0° to +45 and to -45° and 1° increment from +45°/-45° to +70°/- 70°.

Magnification 19000x.

Defocus -5 µm

Total dose = 100 $e^{-}.Å^{-2}$

PEO_{39}-*b*-$PODMA_{17}$ at 45 ˚C:

From -70° to +67°, with 2° increments from 0° to +45 and to -45° and 1° increment from +45°/-45° to +67°/- 70°.

Magnification 15000x.

Defocus -5 µm

Total dose = 100 $e^{-}.Å^{-2}$

5wt% solution PEO_{39}-*b*-$PODMA_{17}$

PEO_{39}-*b*-$PODMA_{17}$ at 4 ˚C:

From -65° to +65°, with 1.5° increments.

Magnification 19000x.

Defocus -10 µm

Total dose = 40 $e^{-}.Å^{-2}$

PEO_{39}-*b*-$PODMA_{17}$ at 45 ˚C:

From -66° to +66°, with 1.5° increments.

Magnification 11500x.

Defocus -15 µm

Total dose = 40 $e^{-}.Å^{-2}$

Supporting Information

Syntheses

Preparation of Ethylene Glycol Methyl 2-Bromo 2-Methyl Propanoate (PEO macroinitiator)

A modification of a literature method was followed.[2] A solution of PEGME M_n ca. 2000 $gmol^{-1}$ (10g, 5 mmol) in dichloromethane was added dropwise to a stirred mixture of 2-bromoisobutyryl bromide (1.24ml, 10 mmol), triethylamine (1.4ml, 10 mmol), and dimethylamino pyridine (1.22g, 10 mmol) in dichloromethane at 0˚C for 1h under nitrogen. The solution was stirred for a further 18 h at room temperature. A third of the reaction solvent was evaporated off and the resultant yellow precipitate was filtered off. The remaining solution was made up to 100ml with dichloromethane and transferred to a separating funnel. The solution was washed several times with a saturated sodium bicarbonate solution and then with a 10% hydrochloric acid solution. The organic layer was collected and dried over anhydrous magnesium sulphate for an hour, filtered and the dichloromethane evaporated off. Finally, the resultant yellow solid was left in the vacuum oven at 50^{o}C for two hours.

The structure was confirmed using ^{1}H, ^{13}C NMR and Fourier Transform Infrared (FTIR) spectroscopy, and molecular weight parameters calculated using size exclusion chromatography (SEC).

^{1}H NMR (270 MHz, $CDCl_3$, ppm) δ: 1.80 (singlet, 6H, $(CH_3)_2C$-), 3.36 (singlet, 3H, -OCH_3), 3.59 (broad peak, 4H -OCH_2CH_2-), 3.84 (triplet, 2H, –CH_2O-), 4.28 (triplet, 2H, O=$COCH_2$-). **^{13}C NMR** (270 MHz, $CDCl_3$, ppm) δ: 30.75 [$(CH_3)_2$], 55.69 (C-Br), 59.03 (-OCH_3), 65.13 (O=$COCH_2$-), 68.73 (-CH_2O-), 70.57 (-CH_2CH_2O-), 71.92 (-CH_2-OCH_3), 171.59 (–C=O). **FTIR** (cm^{-1}): 2882.9 (strong peak C-H stretches), 1734.5 (moderate peak C=O), 1146.6 (weak peak C-O ester stretch), 1099.9 (strong peak C-O ether stretches), 528.3 (weak peak C-Br).

Preparation of PEO_{39}-b-$ODMA_{17}$

The block copolymer was synthesised via ATRP[3] as follows: The PEO macroinitiator (0.84g, 0.44 mmol) was placed in a schlenk tube along with a magnetic stirrer, and dissolved in 2ml of a solution of xylene with 10% isopropanol. To this solution were added octadecyl methacrylate (also dissolved in 2 ml of the above solution) (2.5g, 7.4 mmol), N-(n-octyl)-2-pyridyl(methanime) (0.19g, 0.88 mmol) and Cu(I)Br (22.5mg, 0.16 mmol). The schlenk tube was then sealed and the solution degassed with nitrogen for 30mins. The reaction mixture was placed in an oil bath at 95˚C for 48 hours. The reaction mixture was then exposed to air, diluted in THF and run through an alumina column. The polymer was isolated from precipitation into methanol.

The structure was confirmed using ^{1}H, ^{13}C NMR and FTIR spectroscopy, and molecular weight parameters calculated using SEC.

^{1}H NMR (270 MHz, $CDCl_3$, ppm) δ: 0.88 (broad peak, 3H, –$(CH_2)_{17}$-CH_3), 1.03-1.4 (broad peaks, CH_3-C-CH_2- and -CH_2-$(CH_2)_{15}$-), 1.26 (broad peak, 30H -$(CH_2)_{15}$-), 1.53-2.10 (broad peaks, CH_3-C-CH_2-), 3.38 (singlet, 3H –OCH_3 PEO), 3.64 (broad peak, 4H –(OCH_2CH_2)-PEO), 3.91 (broad peak, 2H, O=CO-CH_2). **^{13}C NMR** ($CDCl_3$, ppm) δ: 14.05 (-**C**H_3); 18.26 (CH_3-C-CH_2-); 25.99 (-$OCH_2CH_2CH_2$); 28.12 (-OCH_2CH_2-); 29.35 (-$CH_2(CH_2)_{10}CH_2$-); 29.68 (-(**C**$H_2)_{10}$-); 31.86 (-$CH_2CH_2CH_3$); 64.92 (-OCH_2-); 70.51 (-(O**C**H_2**C**H_2)-). **FTIR** (cm^{-1}): 2916.0-2849.0 (strong peaks C-H stretches), 1726.5 (strong peak, C=O), 1146.0 (moderate peak C-O stretches).

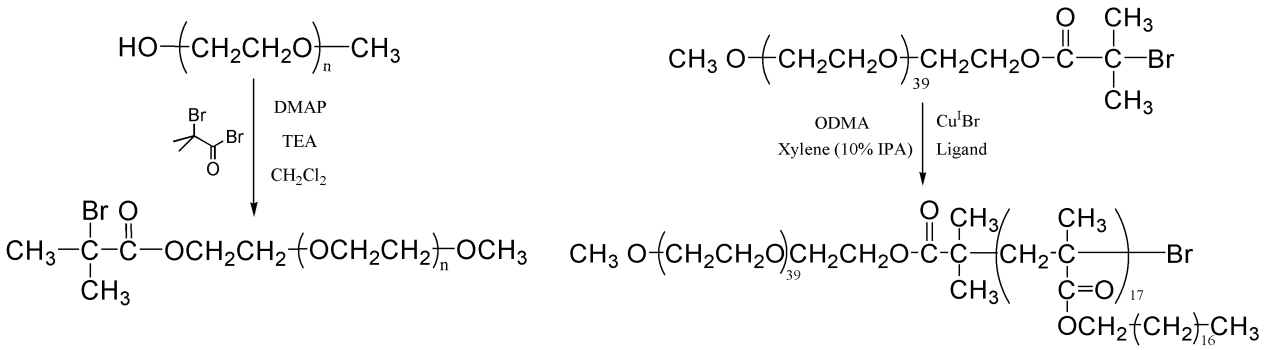

Scheme S1: Synthesis of PEO macroinitiator and PEO-PODMA block copolymer.

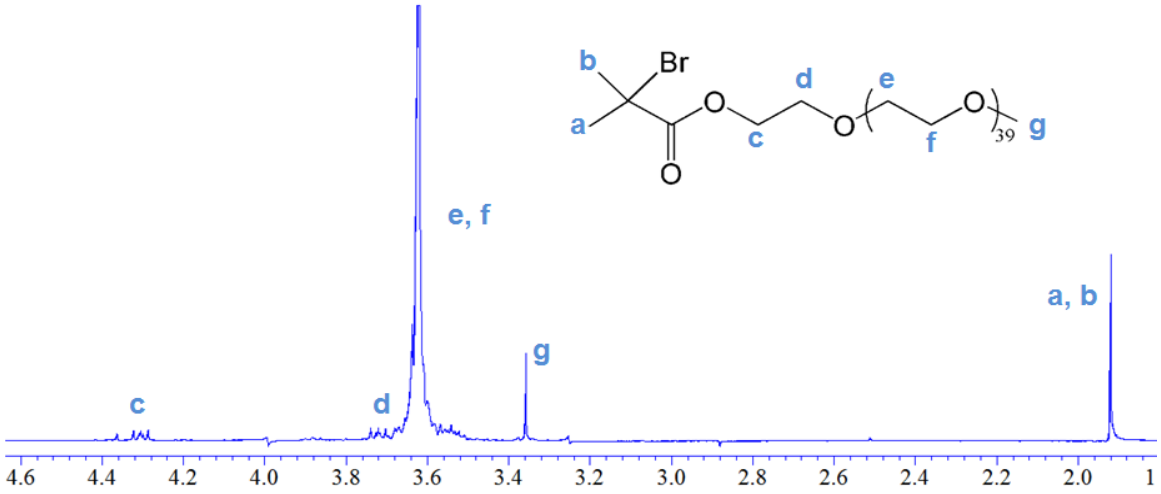

Figure S1: ^{1}H NMR spectrum of the PEO macroinitiator in $CDCl_3$.

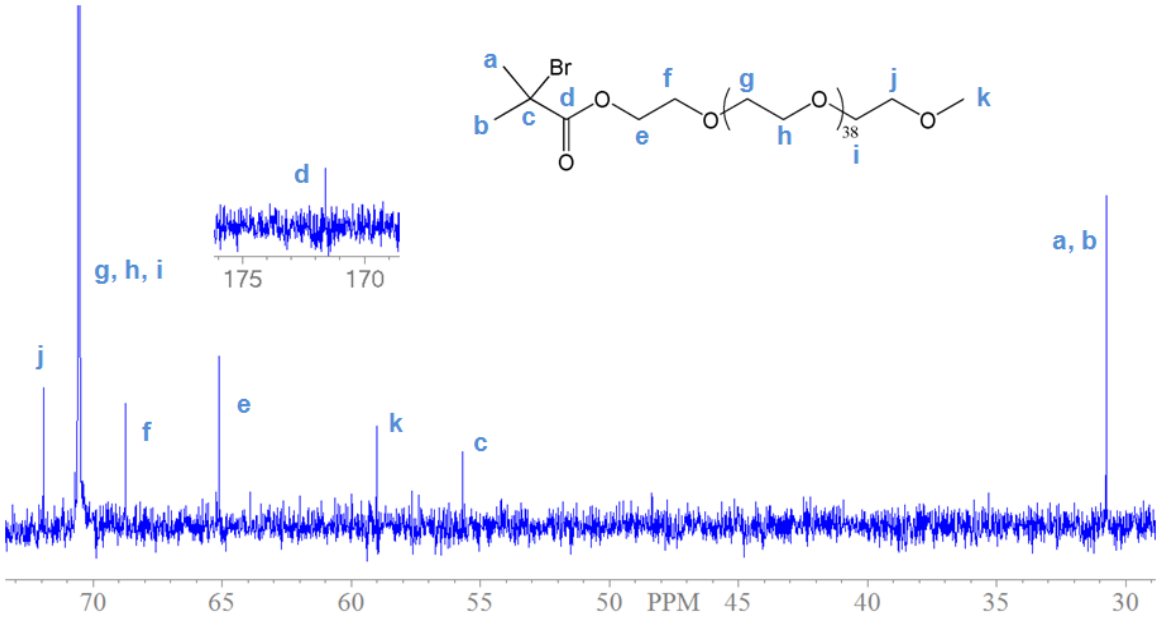

Figure S2: ^{13}C NMR spectrum of the PEO macroinitiator in $CDCl_3$.

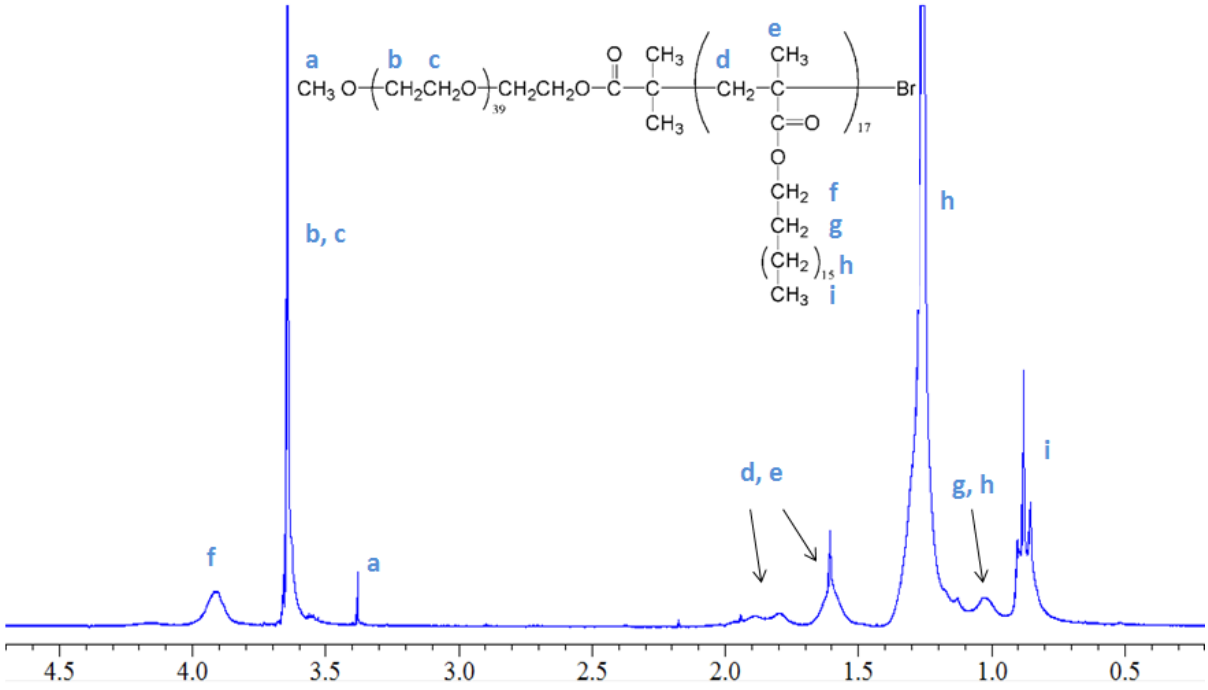

Figure S3 : ^{1}H NMR spectrum of PEO_{39}-*b*-$PODMA_{17}$ in $CDCl_3$.

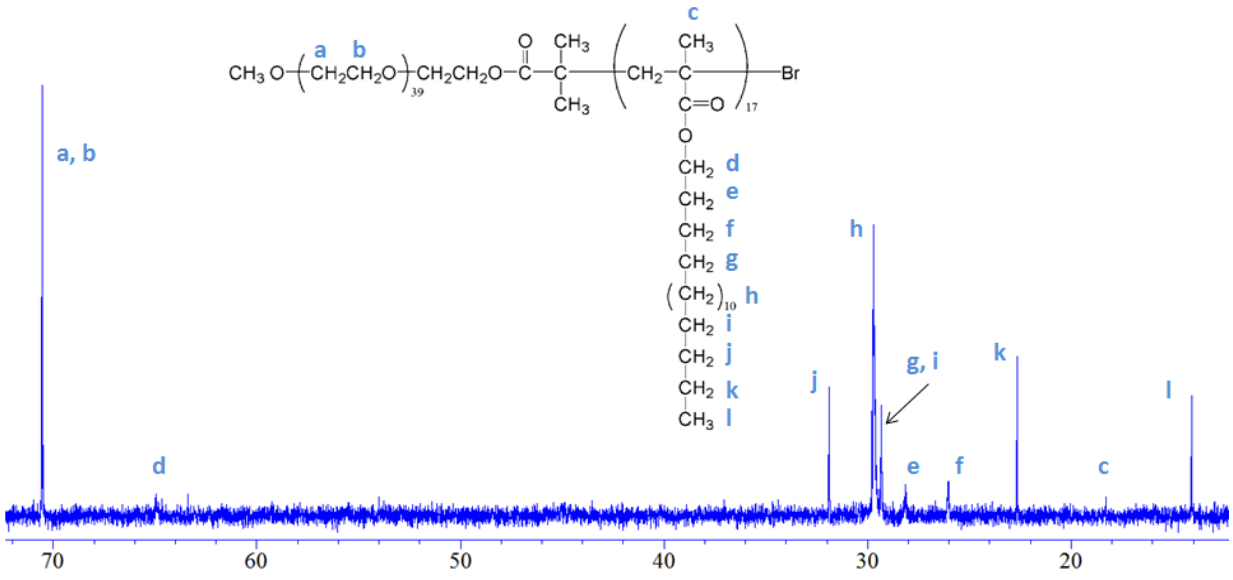

Figure S4: ^{13}C NMR spectrum of PEO_{39}-*b*-$PODMA_{17}$ in $CDCl_3$.

SI2 DSC

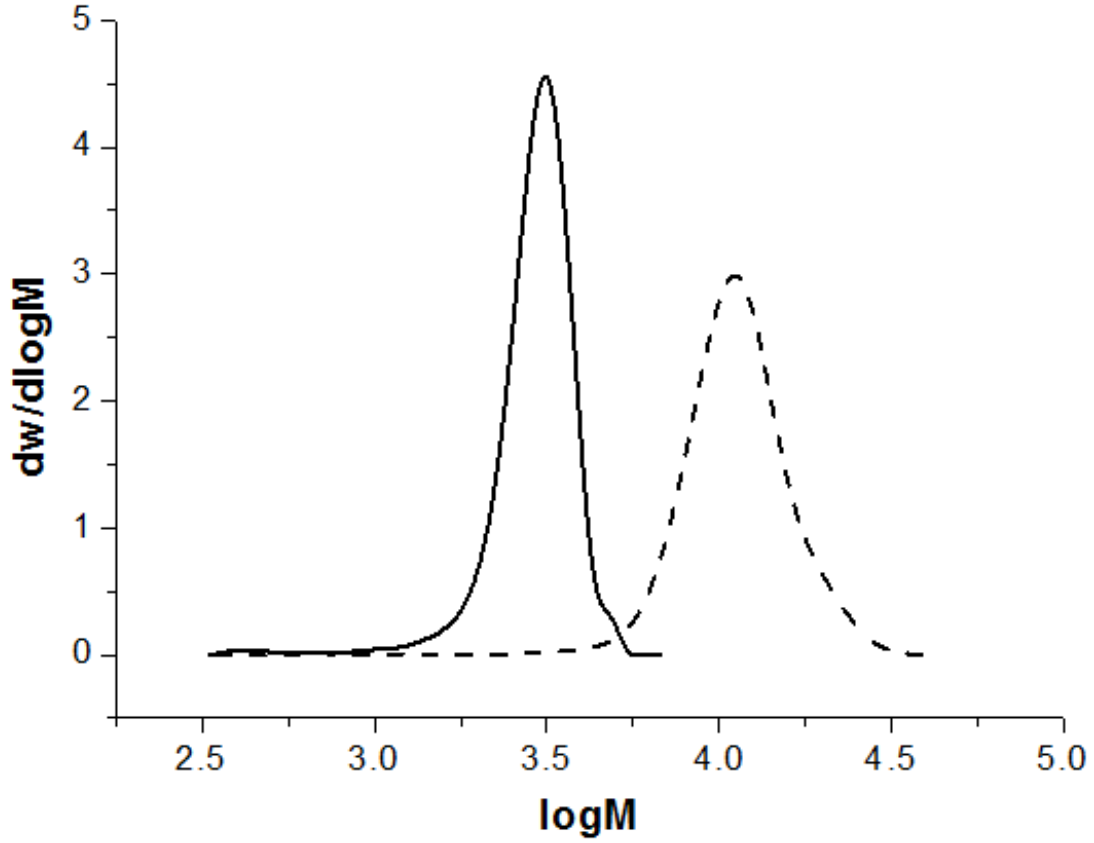

Figure S5: SEC traces of the PEO macroinitiator and PEO_{39}-*b*-$ODMA_{17}$.

Table S1: Molecular weight parameters of PEO and PEO_{39}-*b*-$PODMA_{17}$.

	M_n *a*	M_n *b*	M_w *b*	M_w/M_n *b*
PEO Macroinitiator	1,934	2,846	3,020	1.06
PEO_{39}-*b*-$PODMA_{17}$	7,680	10,754	11,937	1.11

a: calculated via ^{1}H NMR spectroscopy
b: calculated via SEC

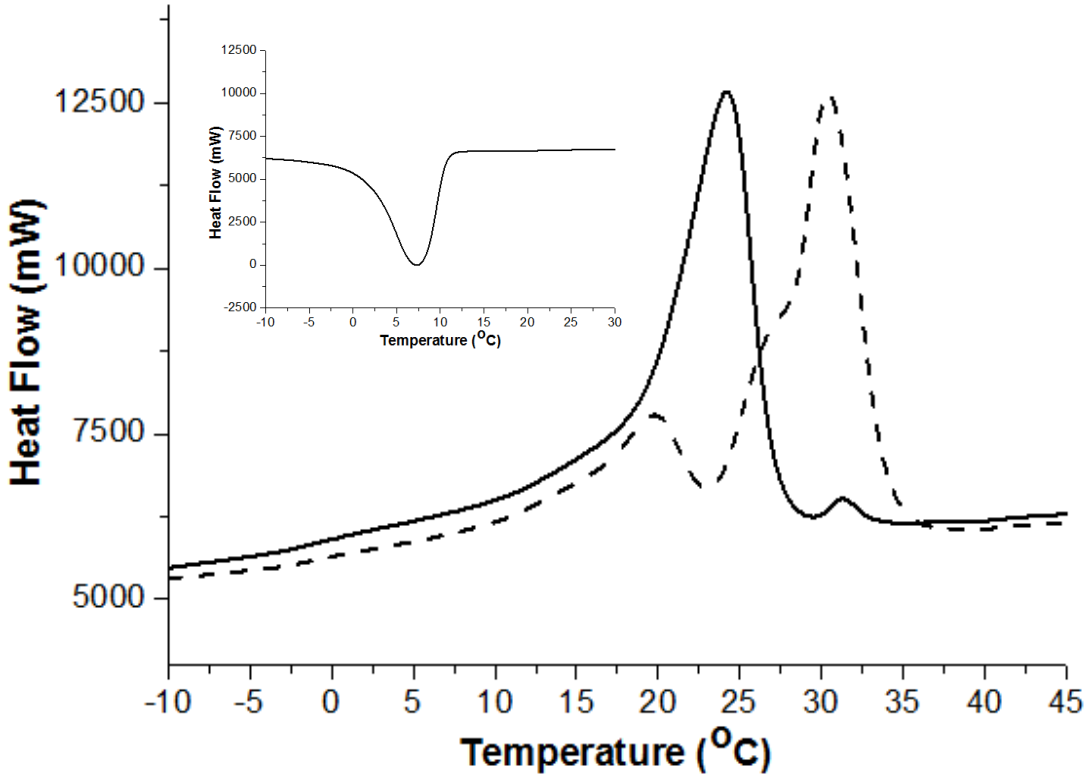

Figure S6: DSC scans of PEO_{39}-*b*-$PODMA_{17}$ (in bulk) measured during ···· 1st heating and —— 2nd heating runs. Inset, crystallisation during cooling (Tc)

Discussion of DSC Results

Thermal analysis of the polymer was carried out using DSC (Figure SI6). Analysis of the separate semi-crystalline components displayed melting transitions with T_{onset}= 17.4°C (ΔH = 39.7 Jg^{-1}) and 40.5°C (ΔH = 141.6 Jg^{-1}) for PODMA (DP=45) and the PEO macroinitiator (PEO = 39 units), respectively. Whereas the PEO transition is in agreement with literature values, the PODMA melts at a considerably lower value than reported for higher MW samples (e.g. Tm = 39°C for PODMA Mn=210,000),[4,5] most likely a consequence of its low molecular weight inhibiting extensive crystallisation.

The initial heating run revealed two melting transitions at 19.8°C and 30.4°C possibly corresponding to the PODMA and PEO blocks respectively. This is due to a temporary separation of the PEO and PODMA components of the block copolymer, probably induced by the precipitation of the polymer into methanol during its purification (PEO being more soluble in methanol than PODMA). This first heating run was therefore used to eradicate the thermal behaviour induced by environmental/ experimental exposure. The sample was then cooled at a rate of -10°C/min and crystallisation occurred at 7.3°C, which closely corresponds to the T_c of the $PODMA_{45}$ homopolymer at 8°C.

The second heating run for PEO_{39}-*b*-$PODMA_{17}$ showed two melting transitions: a large transition with T_{onset} =18.2, (ΔH = 38.3 Jg^{-1}) and a very small transition with T_{onset} =29.9, (ΔH = 0.45 Jg^{-1}) which were attributed to the PODMA and PEO blocks, respectively. The data for the PODMA block are very similar to those recorded of the pure component, indicating a microphase separated structure before the transition. In contrast, the low melting enthalpy recorded for the PEO block suggests that only a very small fraction of the PEO exists in a microphase separated state after PODMA melting. Hence the two polymer blocks become miscible above ~18°C.

SI3 DLS

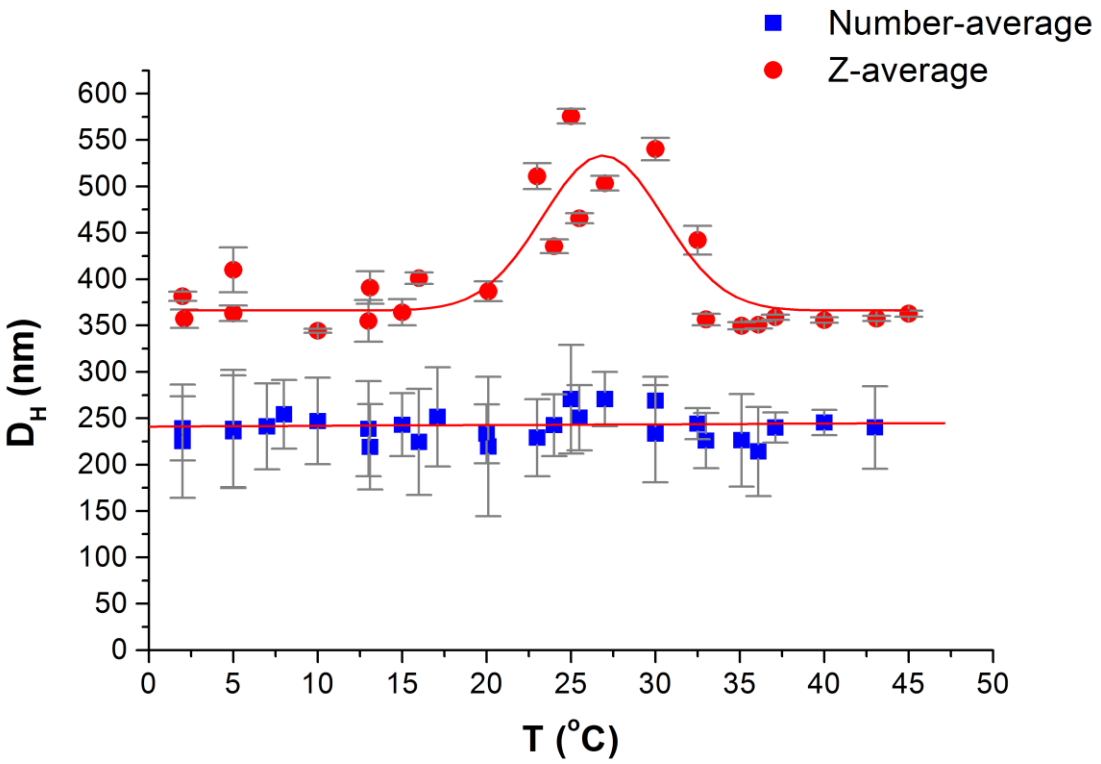

Figure S7: Number and z-average particle diameters of PEO_{39}-*b*-$PODMA_{17}$ aggregates taken with increasing temperature. Each size measurement was obtained from an average of ten readings at each temperature. Error bars represent the standard deviation of the hydrodynamic diameter (D_H) recorded at each temperature.

SI4 CryoTEM

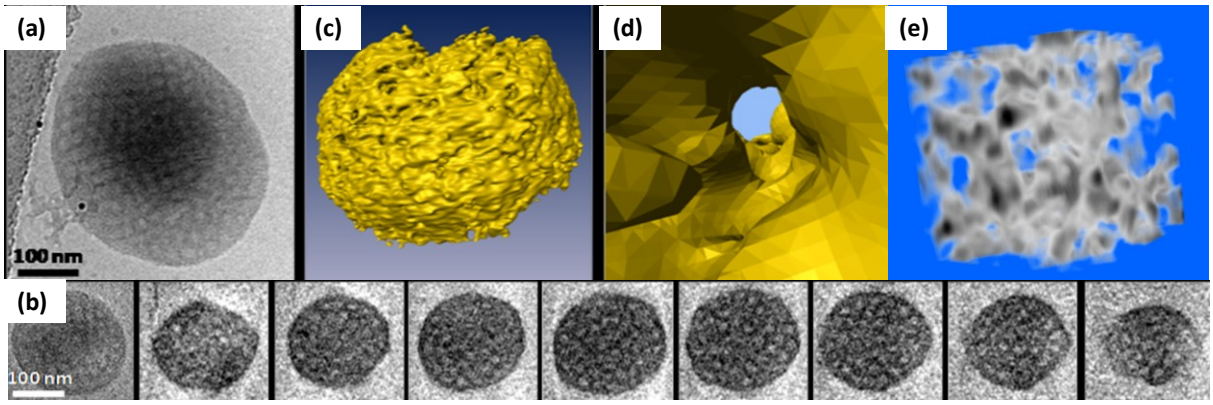

Figure S8: cryoTEM of 1wt % solution of PEO_{39}-*b*-$PODMA_{17}$ aggregates at 4°C : (a) 2D projection image of a larger aggregate; (b) gallery showing an 2D projection image (1st image) of a smaller aggregate and z slices of a 3D reconstruction of a tilt series of the same particle; (c-e) computer aided visualization of the reconstruction in (b) showing (c) the shape of the aggregate, (d) the connection of the internal structure with the surrounding solution and (e) the bicontinueous nature of the internal aggregate structure.

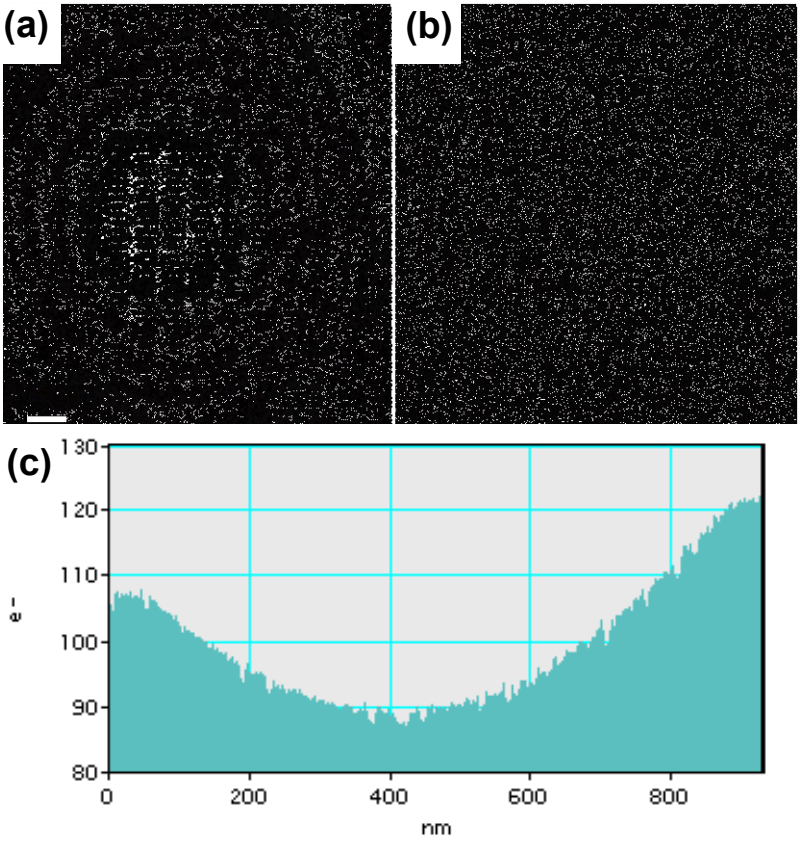

Figure S9: cryoTEM of 1wt % solution of PEO_{39}-*b*-$PODMA_{17}$ aggregate at 45°C: (a) 2D projection image of one of the aggregates, darks spots are gold nanoparticles used as fiducial markers for tomography; (b) z-slice of a 3D reconstruction of a tilt series of the same particle, showing the internal aggregate structure; (c) electron density profile through the aggregate in (a)

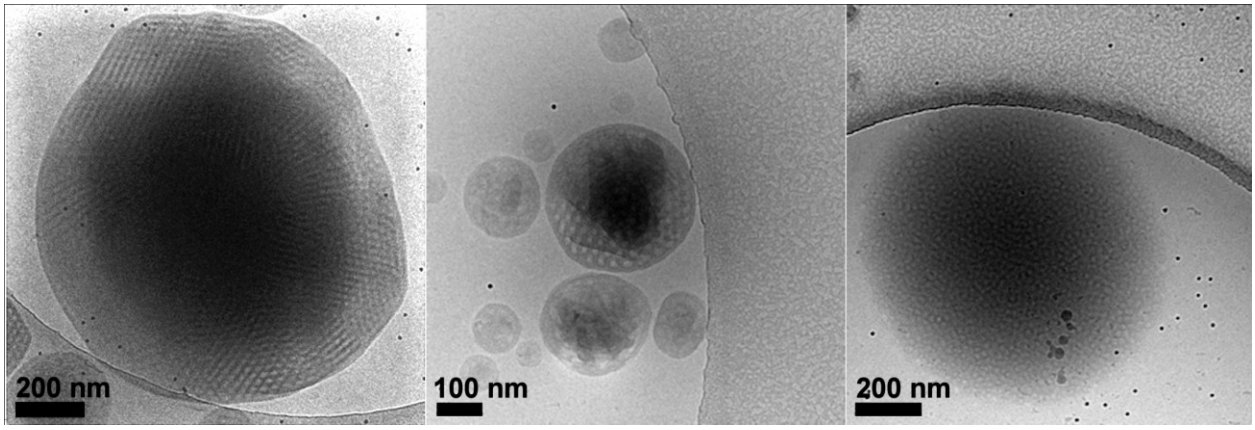

Figure S10: cryoTEM 2D projection images of 5wt % solution of PEO_{39}-*b*-$PODMA_{17}$ aggregates vitrified at (a) 4 ^{o}C, (b) 22 ^{o}C and (c) 45 ^{o}C.

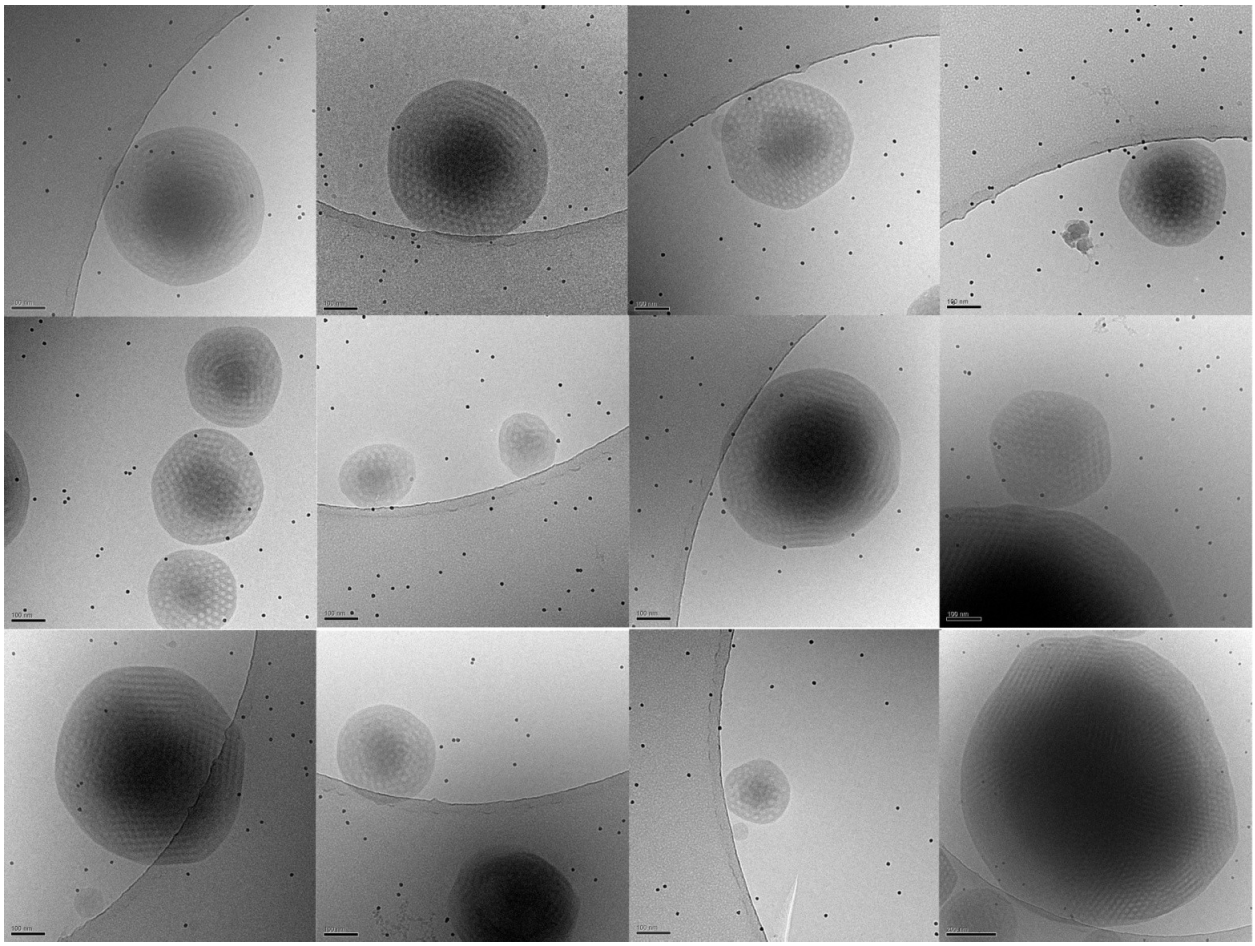

Figure S11: cryoTEM 2D projection images of 5wt % solution of PEO_{39}-*b*-$PODMA_{17}$ aggregates vitrified at 4 ^{o}C,

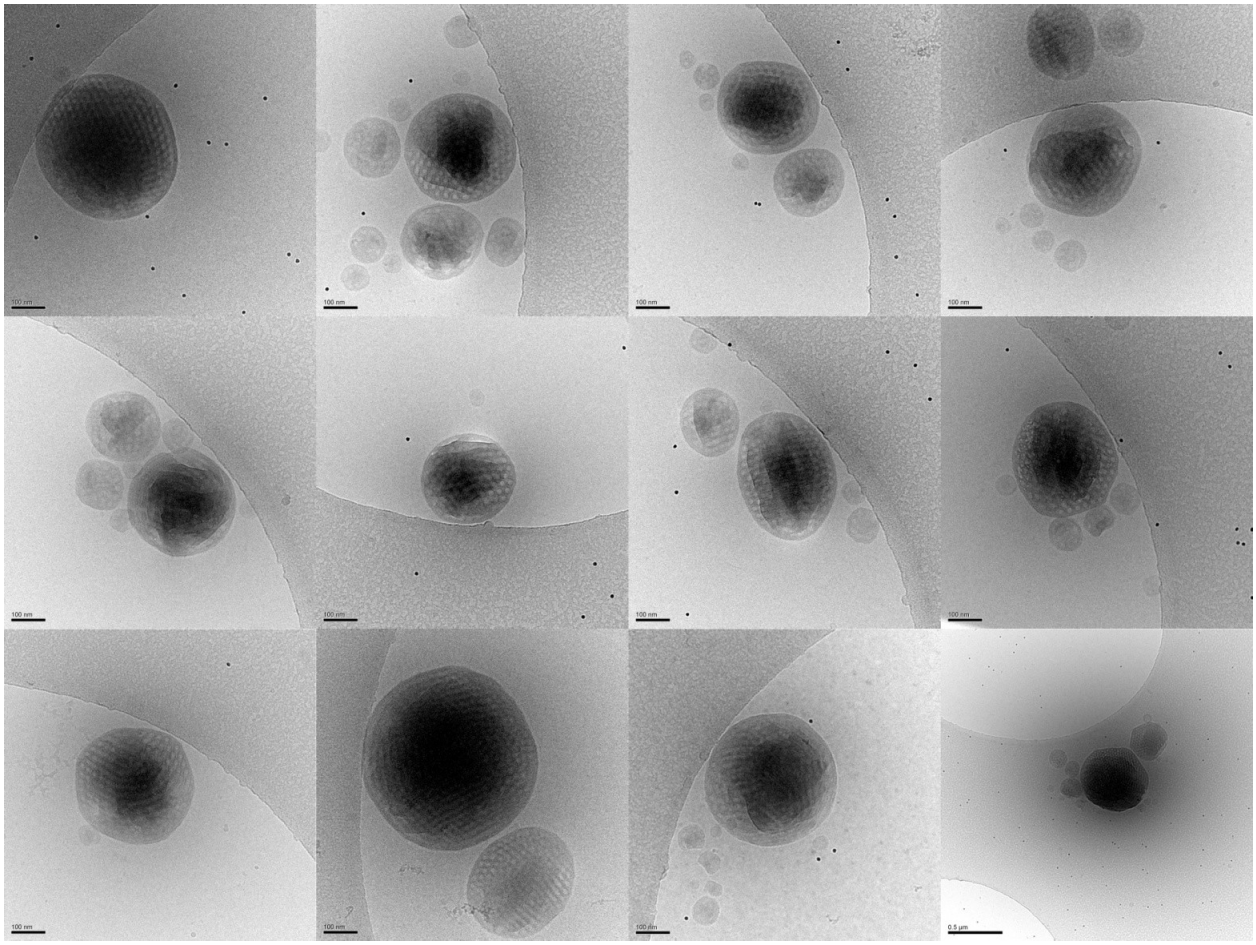

Figure S12: cryoTEM 2D projection images of 5wt % solution of PEO_{39}-*b*-$PODMA_{17}$ aggregates vitrified at 22 ^{o}C,

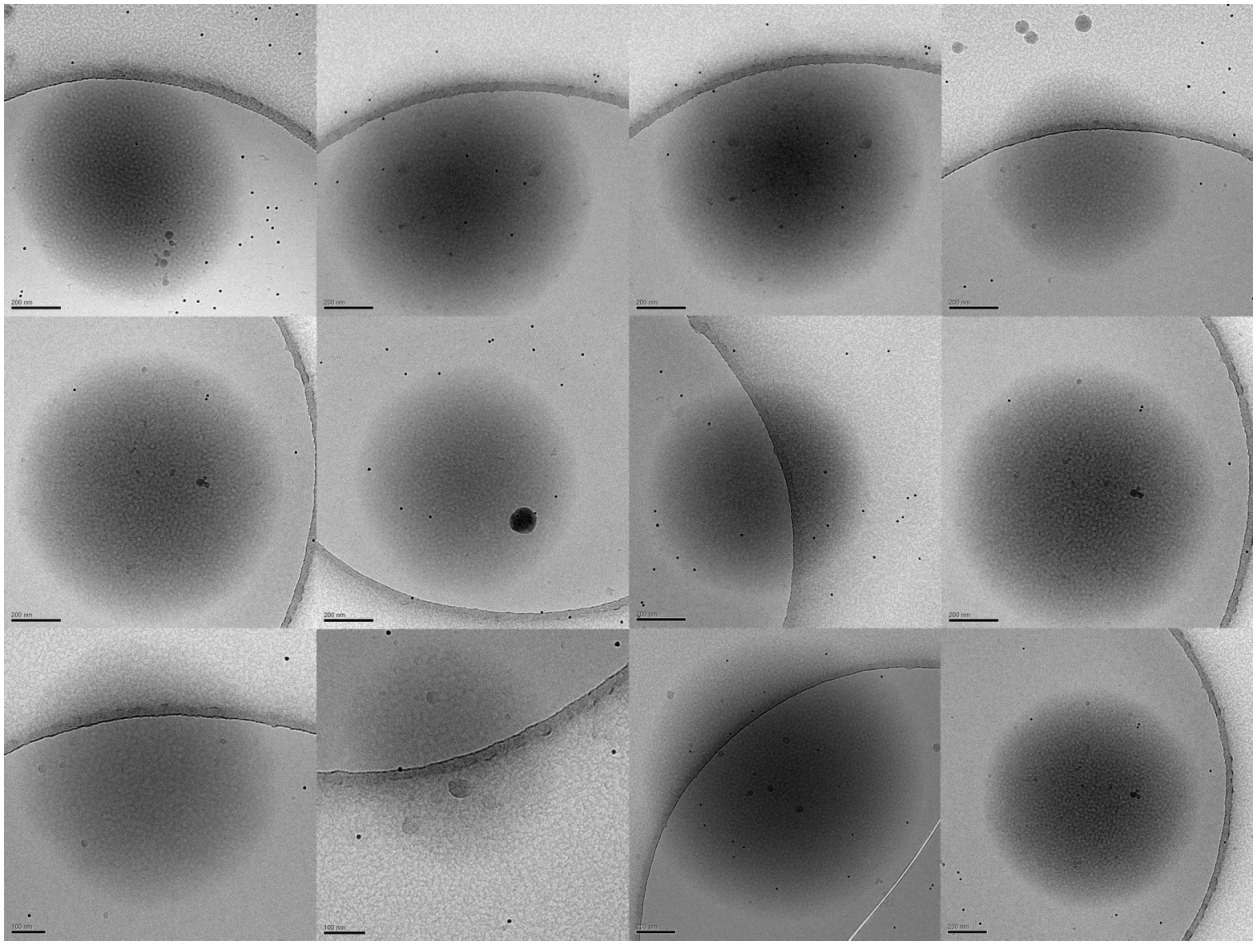

Figure S13: cryoTEM 2D projection images of 5wt % solution of PEO_{39}-*b*-$PODMA_{17}$ aggregates vitrified at 45 ^{o}C,

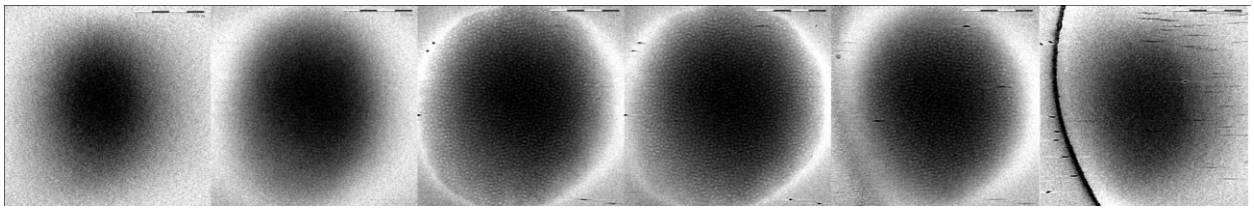

Figure S14: cryoET of a 5wt % solution of PEO_{39}-*b*-$PODMA_{17}$ aggregates at 45°C : gallery of z slices (top to bottom, left to right) of a 3D reconstruction of a tilt series of a particle showing its internal structure.

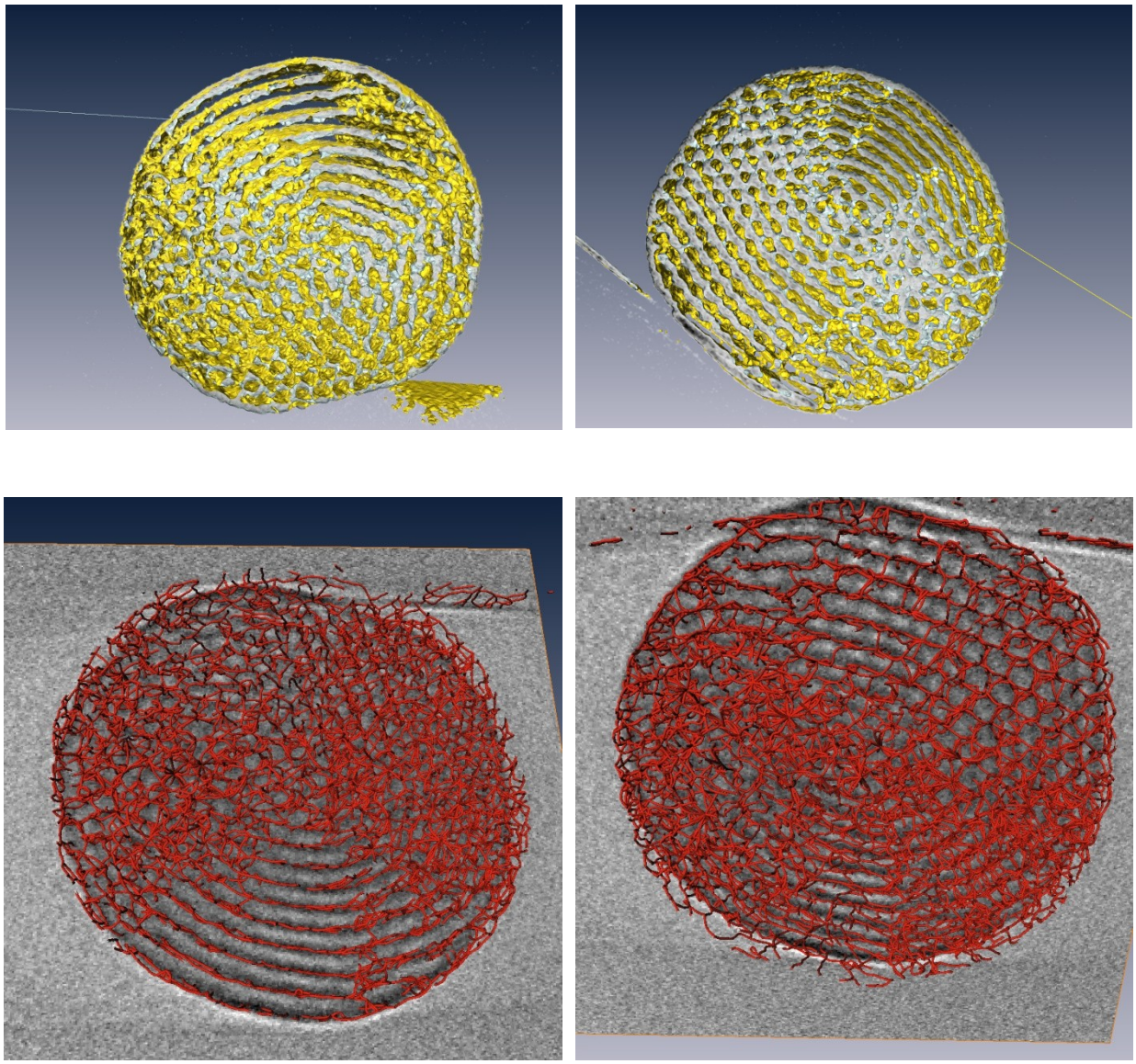

Figure S15: cryoET of 5wt % solution of PEO_{39}-*b*-$PODMA_{17}$ aggregates at 4°C: (top) computer aided visualization of a cryoelectron tomograms under different angles showing the coexistence of lamellar and bicontinuous regions; (bottom) overlays of a cross-section of the 3D reconstruction and the skeletonised view on the organic material (corresponding to the top images) showing the bicontinuous structure.

SI5 Incorporation of pyrene

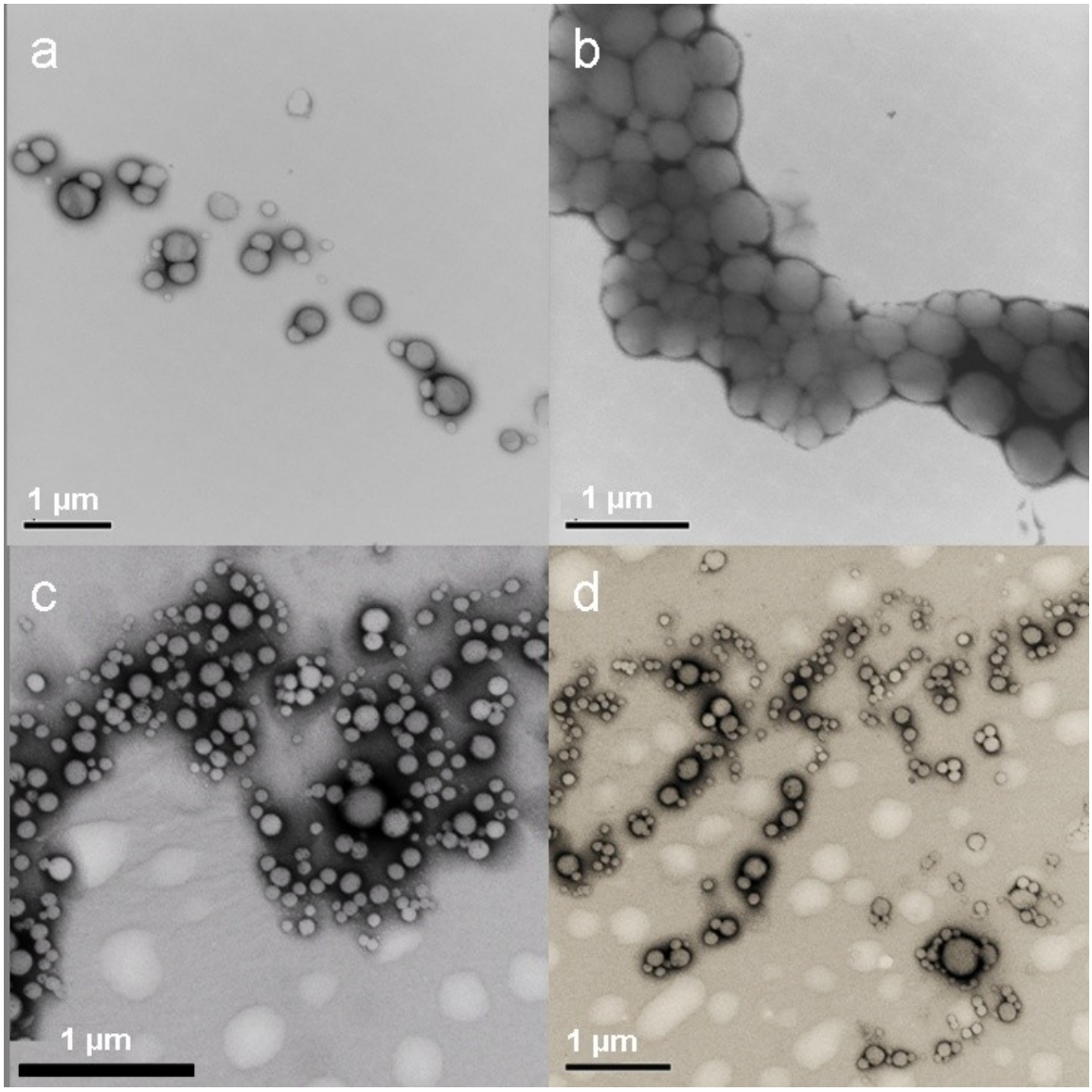

Figure S16: Negative staining TEM pictures of 1 wt% PEO_{39}-*b*-$PODMA_{17}$ aggregate solutions: (a) and (b) without pyrene; (c) and (d) with pyrene.

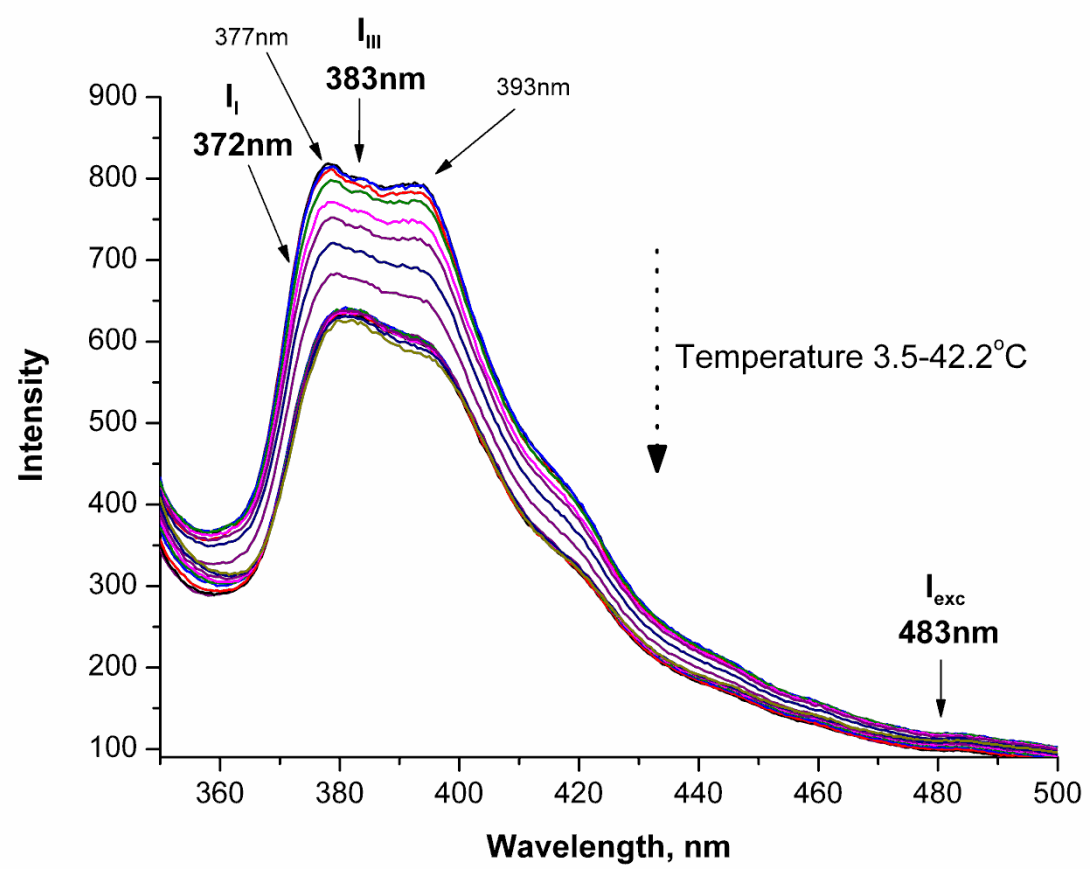

Figure S17: Fluorescence spectra at various temperatures for pyrene encapsulated in PEO_{39}-*b*-$PODMA_{17}$ micelles with significant fluorescence peaks labelled.

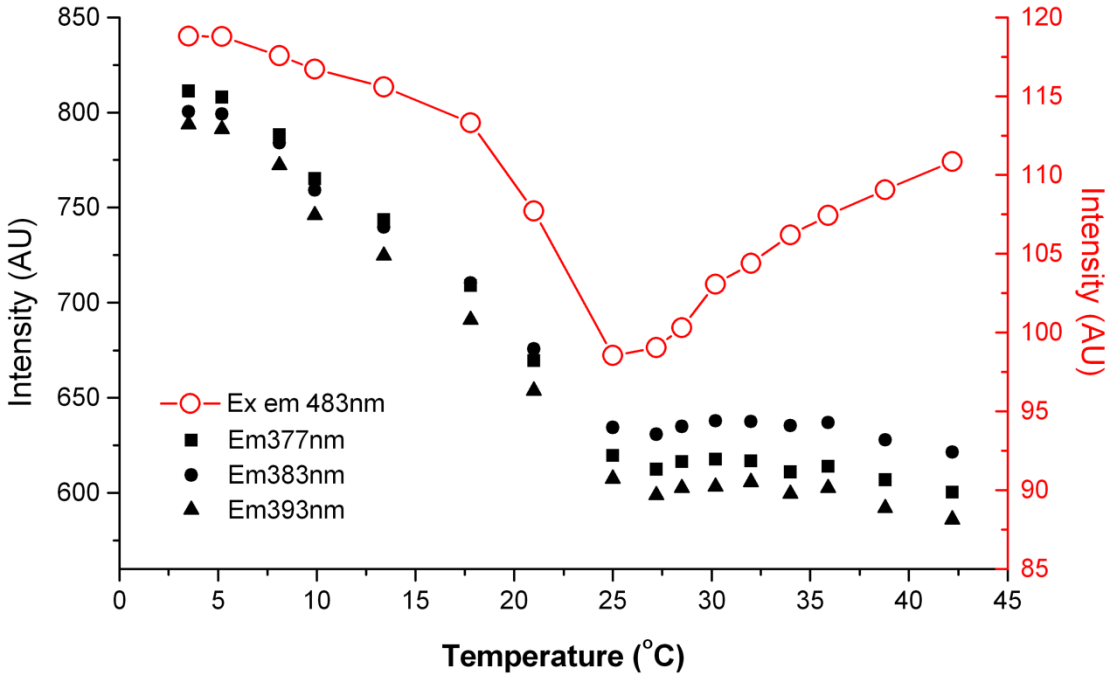

Figure S18: Variation with temperature of ratios of the I_{III}:I_I (I_{Em383}/I_{Em372}) bands and the I_{exc}:I_{mon} (I_{Ex483}/I_{Mon372}) bands of pyrene encapsulated in PEO_{39}-*b*-$PODMA_{17}$ micelles.

References:

1. Haddleton, D. M.; Jasceczek, C. B.; Hannon, M. J.; Shooter, A. J. *Macromolecules*, **1997**, 30, 2190-2193.
2. Jankova, K.; Chen, X.; Kops, J.; Batsberg, W. *Macromolecules,* **1998**, 31, 538-541.
3. G. Street, D. Illsley, S. J. Holder; *J. Polym. Sci: Pt A: Polym. Chem.* **2005,** 43, 1129-1143.
4. Mogri, Z.; Paul, D. R. *Polymer* **2001**, 42, 7765-7780.
5. (a) Sánchez-Soto1, P. J.; Ginés, J. M.; Arias, M. J.; Novák, Cs.; Ruiz-Conde, A. *J. Therm. Anal. Calor*. **2002**, 67, 189-197. (b) Afifi-Effat, A. M.; Hay, J. N. ***Chem. Soc., Faraday Trans. 2*** **1972**, 68, 656 – 661.